Rev. Roum. Sci. Techn.– Électrotechn. et Énerg.
Vol. **71**, *1*, pp. 53–58, Bucarest, 2026

ENHANCING WIND FARM PERFORMANCE THROUGH A PARTICLE SWARM-BASED OPTIMIZATION OF TURBINE DIMENSIONS AND LAYOUT

MOURAD NAIDJI[1*], ALLA EDDINE TOUBAL MAAMAR[2], MOURAD DAFRI[3],
MOHAMED ILYAS RAHAL[4], RADU-FLORIN PORUMB[5]

Keywords: Wind turbine; Rotor diameter; Hub height; Windfarm configuration; Particle swarm optimization (PSO) algorithm; Cost estimation; Efficiency.

Wind energy plays a crucial role in the global transition toward sustainable power generation. To meet the growing demand for renewable energy, optimizing wind farm design is essential for both maximizing energy output and minimizing costs. This paper builds upon previous studies by refining and expanding several ideal wind turbine configurations, using them as the foundation for a more comprehensive analysis and enhancement. While prior research has primarily focused on reducing the cost per kilowatt (cost/kW) of power generated, this study takes a broader approach, aiming to optimize overall wind farm efficiency through the strategic adjustment of turbine rotor diameters and hub heights. By implementing a particle swarm optimization (PSO) algorithm, this work identifies the optimal arrangement of these turbine dimensions to achieve higher efficiency while simultaneously reducing overall costs. The proposed methodology offers a flexible, scalable solution that can significantly enhance wind farm performance, making it more adaptable to varying environmental conditions and economic constraints.

1. INTRODUCTION

The global energy sector is undergoing a rapid transformation as countries strive to meet ambitious renewable energy source (RES) targets and reduce greenhouse gas emissions [1]. Within this context, wind energy has emerged as one of the most mature and cost-effective renewable technologies. However, achieving high energy yield while maintaining economic viability remains a major challenge, making wind farm design optimization a critical research topic.

Wind farm performance is strongly influenced by turbine placement and wake interactions. Wake effects caused by upstream turbines reduce the wind speed available to downstream turbines, leading to significant power losses and reduced overall efficiency. As a result, a large body of research has focused on wind farm layout optimization (WFLO), aiming to mitigate wake losses while maximizing power output and minimizing investment or operational costs. Early studies established benchmark optimization frameworks using simplified wake models and cost formulations, which remain widely used for comparative analysis. More recent studies have extended WFLO by incorporating additional physical and economic factors. For instance, cost-oriented optimization approaches emphasize minimizing metrics such as the cost of energy or the levelized cost of energy by balancing turbine placement and investment decisions [2]. Other works investigate the influence of environmental and site-specific parameters, such as elevation height, complex terrain, or offshore conditions, on wind farm performance and economic indicators [3].

Among heuristic optimization techniques, particle swarm optimization (PSO) has been extensively applied to wind farm optimization problems due to its simplicity, fast convergence, and robustness in large-scale, nonlinear search spaces. Numerous PSO-based studies have focused primarily on optimizing turbine layout under fixed turbine characteristics. For example, the authors in [4] proposed a PSO-based framework for determining optimal turbine positions while considering wake effects, achieving measurable improvements in total power output and efficiency. Similarly, the authors in [5] applied PSO to optimize wind farm layout while allowing discrete hub height variations, demonstrating notable gains in both power generation and cost reduction using the Jensen wake model and the Mosetti cost formulation. Recent advances have further enhanced PSO performance through hybridization and algorithmic improvements. Reinforcement learning–based PSO variants have been proposed to overcome premature convergence and improve global exploration, significantly outperforming conventional PSO in layout optimization across multiple wind scenarios [6]. Hybrid approaches combining PSO with artificial neural networks (ANN) have also been developed to exploit historical data and site-specific wind characteristics, yielding substantial improvements in energy extraction efficiency [7]. In addition, PSO has been integrated with genetic algorithms (GA) and CFD-based wind resource assessment to address WFLO in complex terrain [8].

Despite these advances, most PSO-based wind farm optimization studies focus primarily on turbine placement and, in some cases, hub height selection, while assuming uniform rotor diameters across the wind farm. However, turbine dimensions, particularly rotor diameter and hub height, have a direct impact on aerodynamic performance, wake recovery, and capital cost. Several recent works have shown that optimizing hub height jointly with layout can improve wind farm performance, especially when economic factors are considered [9]. Other studies have explored simultaneous optimization of turbine number, hub height, and layout using evolutionary algorithms, demonstrating that multi-parameter optimization yields superior efficiency compared to optimizing individual factors independently [10,11]. Nevertheless, the combined optimization of rotor diameter and hub height within a PSO framework remains relatively underexplored, particularly in the context of heterogeneous turbine configurations within the same wind farm. Most existing approaches either restrict turbine dimensions to a small set of predefined options or focus on

[1] Dept. of Electrical Engineering, Laboratory of Electrical Engineering (LGE), University of M'Sila, Algeria.
[2] LIST Laboratory, University of M'hamed Bougara of Boumerdes, Boumerdes, Algeria.
[3] Dept. of Electrical Engineering, Badji Mokthar-Annaba University. P.O. Box 12, Annaba. 23000, Algeria.
[4] LASA Laboratory, Badji Mokhtar- Annaba University. 12, P.O. Box, Annaba, Algeria.
[5] Laboratory for Efficient Energy Use and Power Quality –LEEUPQ, University Politehnica of Bucharest, Bucharest, Romania.
E-mails: mourad.naidji@univ-msila.dz (*Corresponding author), a.toubalmaamar@univ-boumerdes.dz, mourad.dafri@univ-annaba.dz, mohamed-ilyas.rahal@univ-annaba.dz, radu.porumb@upb.ro

DOI: 10.59277/RRST-EE.2026.1.9

cost-driven turbine size selection without explicitly analyzing wake-induced efficiency improvements.

In response to these gaps, this paper proposes a PSO-based optimization framework that simultaneously optimizes rotor diameters and hub heights while preserving a fixed wind farm layout inspired by well-established benchmark configurations. Unlike conventional PSO-based WFLO studies that assume homogeneous turbine designs, the proposed approach allows for spatially varying turbine dimensions, enabling a progressive adaptation of turbine size along the prevailing wind direction. This technique enhances wake mitigation, improves overall wind farm efficiency, and reduces normalized investment cost without increasing the total number of turbines.

The main contributions of this work can be summarized as follows:

1. A PSO-based optimization framework that jointly optimizes rotor diameter and hub height, extending beyond layout-only or hub-height-only optimization approaches.
2. A refined cost estimation model that incorporates turbine dimension variability, allowing a realistic assessment of cost–performance trade-offs.
3. A comparative analysis with classical benchmark layouts and recent PSO-based studies, demonstrating measurable gains in efficiency and cost-effectiveness.

The remaining sections of this paper are organized as follows: Section 2 presents the mathematical modeling of the wind farm, including wake and cost formulations. Section 3 describes the PSO algorithm and its application to turbine dimension optimization. Section 4 discusses the simulation results and performance comparisons, and Section 5 concludes the paper with final remarks and future research directions.

2. MATHEMATICAL MODELING OF THE WIND FARM

2.1 WIND FARM MODELING

One of the key objectives of wind turbine (WT) location design is to reduce power loss caused by wake interferences among turbines. For an accurate estimation of these losses, a reliable wake model must be utilized. The Jensen model [6], is among the most popular models in the literature. When wind hits a turbine, it decelerates and becomes turbulent and creates a wake, an area of decreased wind speed and heightened turbulence, directly downwind of the turbine.

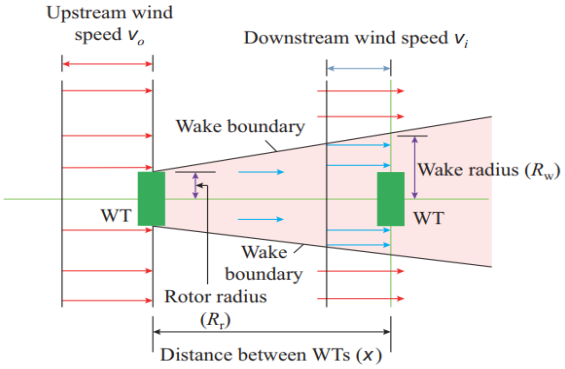

Fig. 1 – Diagram of the "Jensen" wake model.

The wake effect travels downstream and moves sideways, impacting the functioning of downstream turbines. The "Jensen model", as shown in Fig. 1, assumes the wake to increase linearly with downstream distance from the WT and the wind speed profile within the wake to be flat across its cross-section. This is a simplification that makes it computationally inexpensive and therefore suitable for application to large-scale WFLO problems. In this paper, the "Jensen model" is applied in the calculation of the wake velocity deficits, as a basis for the determination of the overall power production from the wind farm. Assuming that the quantity of movement is preserved in the wake section, wind speed can be given as:

$$v = v_0\left[1 - \frac{2a}{\left(1+\alpha\frac{x}{R_r}\right)}\right] \quad (1)$$

$$a = \frac{1-\sqrt{1-C_T}}{2} \quad (2)$$

$$R_r = r\sqrt{\frac{1-a}{1-2a}} \quad (3)$$

$$\alpha = \frac{1/2}{\ln\left(\frac{H}{z_0}\right)} \quad (4)$$

Here, v_0 represents the local wind speed that a turbine experiences when there's no intervention from any wakes. The variable x indicates how far downstream the turbine is located, while R_r refers to the rotor radius of the *WT* that's upstream, and R_w points to the expanded rotor radius of the wake at the downstream site. The hub height is symbolized as H, while α is the entrainment constant, which helps define how quickly the wake expands. The axial induction factor, a, shows how much the wind speed falls due to energy being extracted from the rotor. Additionally, C_T is the thrust coefficient, which measures the force the wind applies on the turbine rotor, and z_0 denotes the surface roughness of the ground in the wind farm area. When a WT is influenced by many upstream wakes, calculating the resulting wake velocity is not as straightforward as just adding them up. Instead, it is generally accepted that the total kinetic energy deficit at the downstream turbine is equal to the sum of the single energy deficits from each wake. Therefore, the effective wind speed that the i-th turbine, situated downstream of N_T turbines, experiences is determined by adding up these energy losses accordingly as:

$$v_i = v_0\left[1 - \sqrt{\sum_{j=1}^{N_T}\left(1 - \frac{v_{ij}}{v_0}\right)^2}\right] \quad (5)$$

The variable v_{ij} denotes the wind speed experienced by the i-th turbine due to the wake generated by the j-th upstream turbine. In the linear wake model, we assume the wake spreads in a conical shape as it travels downstream. The area affected by this wake is defined by the wake influence radius, which indicates how far the wake's impact reaches. This radius is calculated using a specific formula that takes into account the distance between the WTs and the wake decay constant as:

$$R_w = R_r + \alpha x \quad (6)$$

Power output from the i-th wind turbine (WT), expressed in kW, is given by [12]:

$$P_{wt,i} = 0.5\,\rho\,\pi\,r^2\,v_i^3\,C_P/1000 \quad (7)$$

where $P_{wt,i}$ denotes the electrical power produced by the i-th wind turbine while accounting for wake effects, ρ is the air density (kg/m³); (ρ = 1.225kg/m³), r is the rotor radius (m);

v_i is the wind speed at the turbine hub (m/s), and C_P is the power coefficient. For commercial wind turbines, a typical value of $C_P = 0.4$ is assumed.

By substituting the constant parameters, eq. (7) can be simplified as:

$$P_{wt,i} = 0.3v_i^3 \tag{8}$$

The actual power output is regulated according to the available wind speed at any given time and location. This regulation ensures that the turbine does not operate beyond its rated capacity or in unsuitable wind conditions, ensuring both efficiency and safety. The regulation is defined by specific expressions that take into account local wind conditions and operational limits, as stipulated by as follows:

$$P_{wt,i} = \begin{cases} 0 & v_i < 3 \text{ m/s and } v_i > 25 \text{ m/s} \\ 0.3v_i^3 & 3 \text{ m/s} \le v_i < 12 \text{ m/s} \\ 518.4 \text{ kW} & 12 \text{ m/s} \le v_i < 25 \text{ m/s} \end{cases} \tag{9}$$

The above process establishes the cut-in, cut-out, and rated wind speeds, along with the associated output power for each wind turbine (WT), as illustrated in Fig. 2 [13].

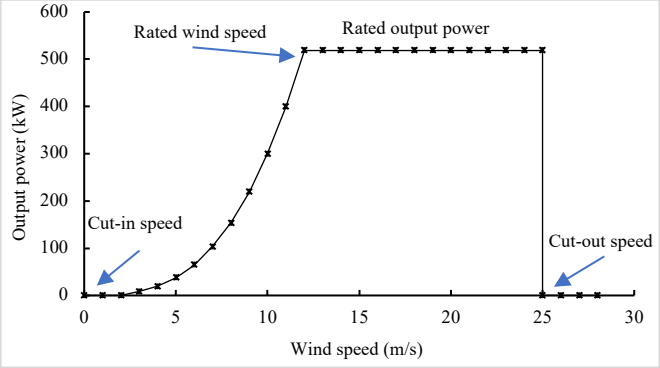

Fig. 2 – Relationship between wind speed and output power for the WT.

2.2 COST ESTIMATION FORMULATION

The cost model presented in [4] considers only a single variable, namely the total number of wind turbines installed in the farm. It is expressed as:

$$Cost_{base} = N\left(\frac{2}{3} + \frac{1}{3}e^{-0.00174N^2}\right), \tag{10}$$

where N denotes the total number of turbines in the wind farm.

This formulation provides a baseline cost estimate but does not account for variations in turbine design parameters such as rotor diameter or hub height. In a conventional wind turbine, the blades and tower represent approximately 17.7% and 21.9% of the turbine cost, respectively [14]. Moreover, the turbine itself typically accounts for about 75% of the total wind farm installation cost [15]. Variations in rotor radius and hub height, therefore, have a non-negligible impact on the overall investment cost. In particular, a 1% change in rotor radius (within ±10% of a reference radius of 20 m) leads to an estimated 3% variation in blade cost [16], while hub cost scales approximately linearly with hub height [17].

To incorporate these design-dependent effects, the baseline cost model is extended by introducing weighted correction terms associated with rotor diameter and hub height variations. The resulting refined cost formulation is given by [18]:

$$Cost = Cost_{base}\left[1 + \frac{1}{N}\sum_{i=1}^{v_1} 0.0039825 x_i N_i + \frac{1}{N}\sum_{j=1}^{v_2} 0.0016425 x_j N_j\right] \tag{11}$$

where:

- $Cost_{base}$ is the baseline cost calculated from eq. (10);
- x_i represents the percentage variation in rotor radius of the i-th turbine variant relative to the reference radius R_{base} =20 m;
- x_j represents the percentage variation in hub height of the j-th turbine variant relative to the reference height H_{base}=60 m;
- v_1 and v_2 represent the number of distinct rotor radius and hub height variants, respectively;
- N_i and N_j are the number of turbines associated with each respective variant.

The numerical coefficients in eq. (11) are obtained through sensitivity analysis and reflect the relative contribution of turbine components to the total wind farm cost.

3. PSO FORMULATION AND APPLICATION

This section discusses the *PSO* principle and its application in the wind farm.

3.1 PARTICLE SWARM OPTIMIZATION (PSO) DESCRIPTION

PSO is an evolutionary computation method inspired by the collective behavior of social organisms. This technique relies on how individual agents make decisions based on two key sources of information. The first is personal experience, each agent evaluates the choices it has previously made, identifying which option has yielded the most favorable outcome and how beneficial it was. The second source of information comes from the experiences of neighboring agents. That is, each agent observes and learns from the performance of others, recognizing which choices have led to optimal results within the swarm and how effective those solutions have been.

Figure 3 shows how a particle in the enhanced PSO algorithm updates its position. The new velocity is computed by merging three components: inertia, memory of the particle's own best position, and cooperation with the global best position found by the intelligence swarm. The particle travels from its actual position to a new position, directed by the present updated velocity. This mechanism can help balance survey and convergence in the optimization course [19].

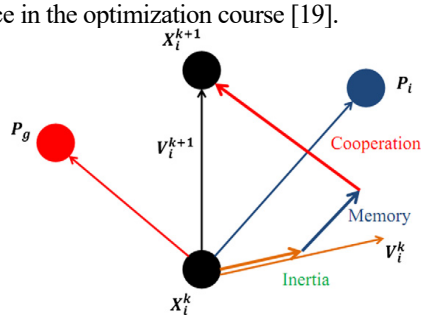

Fig. 3 – Enhanced PSO velocity and position update mechanism.

The particles are controlled according to the following equations:

$$v_i^{t+1} = w^t . v_i^t + c_1 . r_1 . (P_i^t - x_i^t) + c_2 . r_2 . (P_g^t - x_i^t), \tag{12}$$

$$x_i^{t+1} = x_i^t + v_i^{t+1}. \tag{13}$$

Here, i ranges from 1 to N, where N denotes the total

number of individuals in the population. The parameter w represents the inertia weight, which is determined by the following expression:

$$w^t = w_{max} - \left(\frac{w_{max}-w_{min}}{t_{max}}\right) t. \quad (14)$$

3.2 PSO APPLICATION TO WINDFARM CONFIGURATION

For practical implementation, it is neither feasible nor efficient to assign a unique combination of rotor diameter and hub height to every individual turbine in the wind farm. In this study, the evaluated layouts consist of 30 and 26 turbines, respectively, arranged within a 2 km × 2 km wind farm area divided into multiple 200 m × 200 m grid cells. Rather than defining a distinct size for each turbine, three discrete values for rotor diameter and hub height are randomly selected within specified parameter ranges. These values are then systematically and evenly distributed across all turbines in the farm. The rotor diameter is varied between 34 m and 44 m, while the hub height spans from 54 m to 62 m, as input to the PSO algorithm. To simplify computations, the algorithm's selected parameter values are rounded before evaluating the objective function.

Figure 4 illustrates the flowchart of the PSO algorithm, which is employed to determine the optimal WT configuration and dimensions, maximize power output, and minimize associated costs.

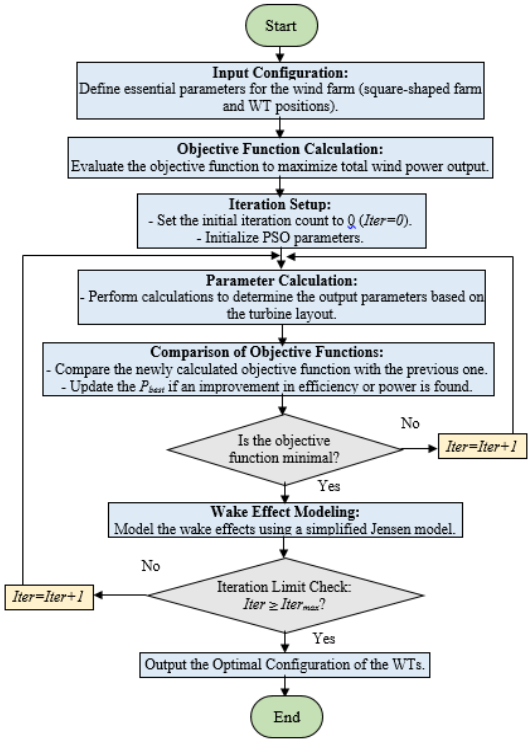

Fig. 4 – Flowchart of the PSO used for optimizing WT configuration.

The power output from each turbine, accounting for wake effects, is computed using eq. (1)-(6). The wind farm's efficiency is defined as:

$$\eta = \frac{\sum_{i=1}^{N} P_{wt,i}}{\sum_{i=1}^{N} P_{wt,max}}. \quad (15)$$

Under this framework, $P_{wt,max}$ represents, assuming no reduction from wake-induced flow deficits, the theoretical peak power output of turbine i.

4. RESULTS AND DISCUSSION

This section presents and discusses the results obtained for two WFLO cases: Case 1, with constant wind speed and constant wind direction, and Case 2, with constant wind speed and variable wind direction. The analysis focuses on wake interactions, power production, efficiency, and economic performance. The wind farm area is discretized into 100 potential turbine locations (cells of 200 m × 200 m). For all simulations, the PSO parameters are selected to ensure fast convergence: inertia weight w=0.5, acceleration coefficients c_1=c_2=2.5, and a maximum of 100 iterations. The random coefficients r_1 and r_2 are uniformly distributed in [0, 1].

4.1 CASE 1: CONSTANT WIND SPEED AND CONSTANT DIRECTION

In Case 1, the WFLO problem is solved for a constant wind speed of 12 m/s with a fixed wind direction from the north (0°). The optimized layout obtained using the proposed PSO-based approach is compared with the results reported in [20], [21], and [4]. All inter-turbine spacing satisfies the rule-of-thumb constraints, ensuring sufficient downstream separation. As a result, direct wake overlap between adjacent turbines is limited, and wake-induced velocity deficits are significantly reduced. This spatial configuration improves the aerodynamic operating conditions of downstream turbines and enhances overall power extraction. Figures 5 and 6 illustrate the optimized configuration for Case 1, highlighting the spatial distribution of rotor diameters and hub heights, respectively. The wind direction indicator is essential for interpreting the progressive variation in turbine dimensions along the wind direction. Larger turbines are preferentially placed in upstream positions, where wind conditions are least disturbed, while smaller turbines are allocated downstream to mitigate wake effects.

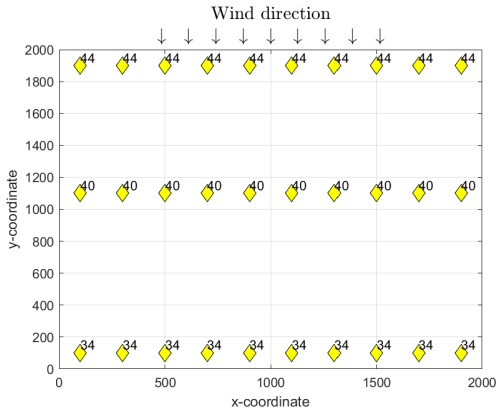

Fig. 5 – Layout indicating optimized rotor diameters for Case 1.

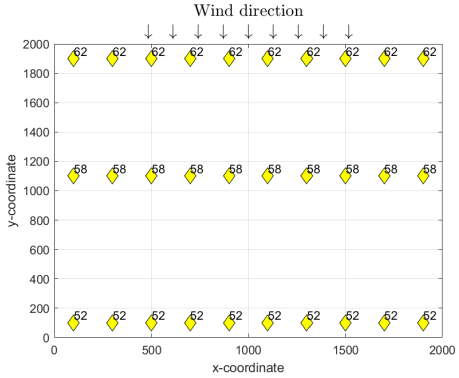

Fig. 6 – Layout indicating optimized hub heights for Case 1.

Table 1 summarizes the performance comparison. With the same number of turbines (30), the proposed method achieves a total power output of 14813 kW and an efficiency of 96.28%, outperforming [20] and [21] in both power output and cost per kilowatt (cost/kW). Although [4] reports higher total power and efficiency, this improvement is achieved by increasing the number of turbines to 32, which directly enhances energy capture but also alters the optimization problem. When normalized by turbine count, the proposed approach demonstrates competitive efficiency while maintaining a lower system complexity and comparable cost performance. Overall, the results indicate that the proposed method provides a balanced trade-off between power generation and economic efficiency without increasing the number of turbines, highlighting the benefit of dimensional optimization over simple capacity expansion.

Table 1

Performance comparison for Case 1

Metric	[20]	[21]	[4]	Proposed
No. of turbines, N	30	30	32*	30
Total power (kW)	14785	14667	16326.59*	14813
Fitness ($\times 10^{-3}$)	1.4940	1.5413	1.4000*	1.4536
Efficiency (%)	95.07	NR	98.42*	96.28

NR: Not reported

* The number of wind turbines is increased/decreased

4.2 CASE 2: CONSTANT WIND SPEED AND VARIABLE WIND DIRECTION

Case 2 represents a more realistic operating scenario in which a constant mean wind speed of 12 m/s is combined with wind directions uniformly distributed over the four cardinal directions (0°, 90°, 180°, and 270°). All turbines are assumed to yaw freely to align with the prevailing wind direction.

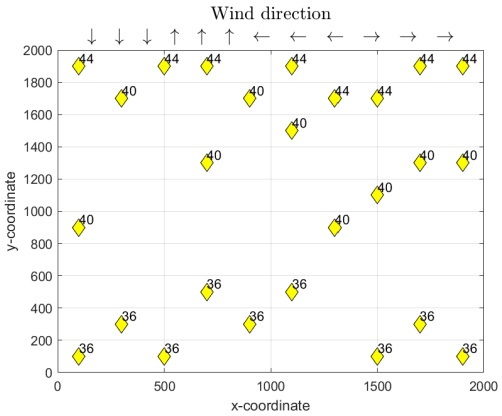

Fig. 7 – Layout indicating optimized rotor diameters for Case 2.

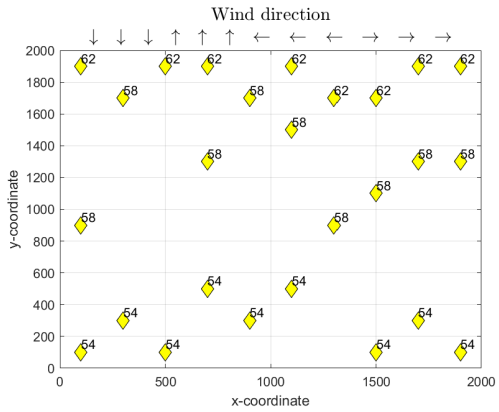

Fig. 8 – Layout indicating optimized hub heights for Case 2.

As wind direction variability increases, the WFLO problem becomes more complex due to changing wake interactions. While the proposed algorithm converges rapidly for individual wind directions, additional iterations are required to obtain stable solutions when multiple wind directions are considered simultaneously. Nevertheless, the final optimized layouts consistently yield improved power output and reduced objective function values. Figures 7 and 8 present the optimized rotor diameters and hub heights for Case 2. Compared to Case 1, the dimensional variations are less directional, reflecting the need to accommodate wakes arising from multiple wind directions rather than a single dominant flow.

Table 2 compares the proposed method with [4,22] and [11]. With 26 turbines, the proposed approach achieves the highest total power output (12990 kW) among methods using the same turbine count and the lowest reported cost/kW.

Table 2

Performance comparison for Case 2

Metric	[22]	[4]	[11]	Proposed
No. of turbines, N	26	19 *	20*	26
Total power (kW)	12980	9741.30 *	10190*	12990
Fitness ($\times 10^{-3}$)	NR	1.6400	1.6346	1.5464
Efficiency (%)	NR	98.90*	97.27	97.45

NR: Not reported

* The number of wind turbines is increased/decreased

Although [4] and [11] report high efficiencies, these results are obtained with fewer turbines (19 and 20, respectively), leading to substantially lower total power generation. The proposed method, therefore, offers superior energy yield while preserving competitive efficiency and economic performance.

4.3 DISCUSSION AND INTERPRETATION OF RESULTS

Across both cases, the optimized layouts follow a clear physical rationale. In Case 1, turbines located in the upstream row employ larger rotor diameters (≈44 m) and higher hubs (≈62 m) to maximize exposure to undisturbed wind. Downstream rows progressively adopt smaller rotors and lower hub heights to compensate for reduced wind speed and increased turbulence. This gradual scaling reflects a deliberate balance between wake mitigation and aerodynamic efficiency. The results in Tables 1 and 2 demonstrate that simultaneous optimization of rotor diameter and hub height significantly improves wind farm efficiency compared with uniform-turbine configurations used in previous studies. Unlike earlier works assuming identical turbines (*e.*g., fixed 20 m rotor radius and 60 m hub height), the proposed approach tailors each turbine to its local flow conditions while keeping the total number of turbines unchanged. Importantly, the method avoids systematic oversizing of turbines. Only upstream turbines are equipped with larger dimensions, while downstream units adopt smaller, cost-effective configurations. This technique enhances power output while limiting unnecessary capital expenditure. Due to the stochastic nature of PSO, the obtained configurations are not unique. Multiple solutions with comparable performance can be achieved, offering flexibility to adapt layouts to site-specific constraints or economic considerations. Using the enhanced cost formulation in eq. (11), the resulting cost/kW ratios confirm that dimensional optimization leads to superior economic performance.

The efficiency trends illustrated in Figs. 9 and 10 further confirm consistent gains over reference studies, emphasizing the role of variable turbine dimensions in reducing wake losses and improving land-use efficiency.

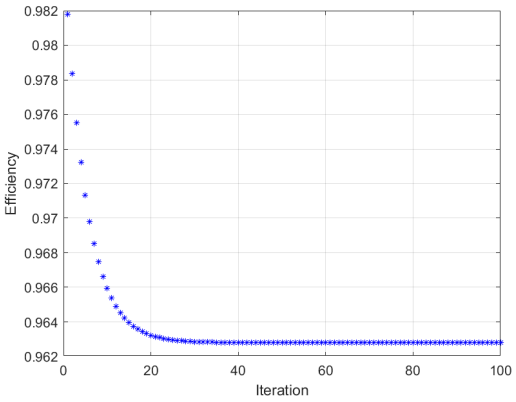

Fig. 9 – Efficiency curve for Case 1.

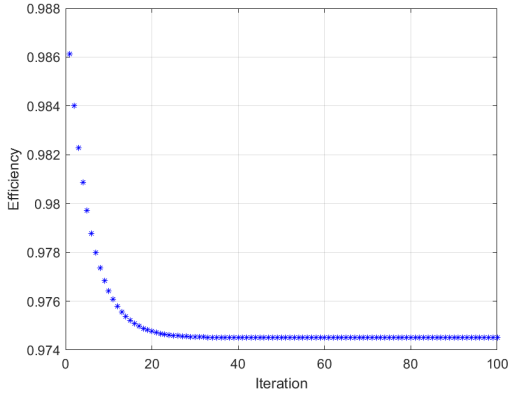

Fig. 10 – Efficiency curve for Case 2.

The proposed method outperforms existing approaches when the turbine count is fixed and remains competitive even when compared against studies that increase the number of turbines. The results confirm that dimensional optimization is an effective alternative to turbine proliferation, yielding measurable gains in efficiency and cost-effectiveness while preserving practical feasibility.

5. CONCLUSIONS

This paper highlights the benefits of optimizing hub heights and rotor diameters in a staggered configuration to improve the efficiency and reduce costs of wind farms, particularly in areas with stable wind conditions. By employing PSO, we have demonstrated that optimizing WT dimensions can lead to enhanced performance. However, the actual impact of these adjustments in more dynamic and complicated situations, such as real-world wind conditions, where wind speed and direction vary simultaneously, remains an area for future exploration. Further research is needed to refine turbine configurations under such variable conditions and to evaluate the long-term benefits of these optimizations across different environmental contexts. Additionally, incorporating other factors such as turbine type and environmental constraints into the optimization process could provide even more robust solutions for future wind farm designs.

CREDIT AUTHORSHIP CONTRIBUTION STATEMENT

Mourad Naidji, Alla Eddine Toubal Maamar, and Mourad Dafri contributed equally to all aspects of the current study, including problem formulation, analysis, and interpretation of results.

Mohamed Ilyas Rahal and Radu-Florin Porumb: equally shared responsibility for the verification of the results and the overall supervision of the research process.

Received on 9 July 2025.

REFERENCES

1. M. Naidji, M. Dafri, A. Laib, *Optimal coordinated voltage control of distribution networks considering renewable energy sources*, ECTI Transactions on Electrical Engineering, Electronics, and Communications, **23**, *1* (2025).
2. P. Ziyaei, M. Khorasanchi, *Effect of cost elements on optimum layout of an offshore wind farm*, Applied Ocean Research, **158**, 104537 (2025).
3. P.S. Portocarrero Mendoza, *Technical-economic evaluation of a 94.5 MW wind power plant at different elevation heights. A case study in Peru's countryside*, Journal of Engineering Research, **13**, *2*, pp. 1089–1103 (2025).
4. P. Asaah, L. Hao, J. Ji, *Optimal placement of wind turbines in wind farm layout using particle swarm optimization*, Journal of Modern Power Systems and Clean Energy, **9**, *2*, pp. 367–375 (2021).
5. M. Yeghikian, A. Ahmadi, R. Dashti, F. Esmaeilion, A. Mahmoudan, S. Hoseinzadeh, D.A. Garcia, *Wind farm layout optimization with different hub heights in Manjil wind farm using particle swarm optimization*, Applied Sciences, **11**, *20*, 9746 (2021).
6. Z. Zhang, J. Li, Z. Lei, Q. Zhu, J. Cheng, S. Gao, *Reinforcement learning-based particle swarm optimization for wind farm layout problems*, Energy, **313**, 134050 (2024).
7. M. El Jaadi, T. Haidi, A. Belfqih, M. Farah, A. Dialmy, *Optimizing wind farm layout for enhanced electricity extraction using a new hybrid PSO-ANN method*, Global Energy Interconnection, **7**, *3*, pp. 254–269 (2024).
8. W. Hu, Q. Yang, Z. Yuan, F. Yang, *Wind farm layout optimization in complex terrain based on CFD and IGA PSO*, Energy, **288**, 129745 (2024).
9. H. Sun, H. Yang, *Wind farm layout and hub height optimization with a novel wake model*, Applied Energy, **348**, 121554 (2023).
10. H. Sun, H. Yang, S. Tao, *Optimization of the number, hub height and layout of offshore wind turbines*, Journal of Marine Science and Engineering, **11**, *8*, 1566 (2023).
11. S.S. Raju M, P. Mohapatra, S. Dutta, R. Mallipeddi, K.N. Das, *Optimal placement of fixed hub height wind turbines in a wind farm using twin archive guided decomposition based multi-objective evolutionary algorithm*, Engineering Applications of Artificial Intelligence, **130**, 107735 (2024).
12. C. Popa et al., *Analysis of wind turbine power output via modeling, simulation, and validation*, Rev. Roum. Sci. Techn. – Électrotechn. et Énerg., **70**, *2*, pp. 175–180 (2025).
13. H. Erol, A. Arslan, *Wind turbine pitch angle control with artificial neural networks*, Rev. Roum. Sci. Techn. – Électrotechn. et Énerg., **70**, *2*, pp. 235–240 (2025).
14. P. Jamieson, *Innovation in wind turbine design*, 2nd ed., Wiley, Chichester (2018).
15. S. Krohn, P.E. Morthorst, S. Awerbuch, *The economics of wind energy*, European Wind Energy Association (EWEA), Brussels, Belgium, pp. 1–156 (2009).
16. F. Fingersh, M. Hand, A. Laxson, *Wind turbine design cost and scaling model*, National Renewable Energy Laboratory (NREL), Tech. Rep. NREL/TP-500-40566 (2006).
17. K. Chen, M.X. Song, X. Zhang, S.F. Wang, *Wind turbine layout optimization with multiple hub height wind turbines using greedy algorithm*, Renewable Energy, **96**, pp. 676–686 (2016).
18. H. Rezk, A. Fathy, A.A.Z. Diab, M. Al-Dhaifallah, *The application of water cycle optimization algorithm for optimal placement of wind turbines in wind farms*, Energies, **12**, *22*, 4335 (2019).
19. M. Naidji, M. Boudour, *Stochastic multi-objective optimal reactive power dispatch considering load and renewable energy sources uncertainties: a case study of the Adrar isolated power system*, International Transactions on Electrical Energy Systems, **30**, *6* (2020).
20. L. Parada, C. Herrera, P. Flores, V. Parada, *Wind farm layout optimization using a Gaussian-based wake model*, Renewable Energy, **107**, pp. 531–541 (2017).
21. M. Beşkirli, İ. Koç, H. Kodaz, *Optimal placement of wind turbines using novel binary invasive weed optimization*, Tehnički Vjesnik, **26**, *1*, pp. 56–63 (2019).
22. S.D.O. Turner, D.A. Romero, P.Y. Zhang, C.H. Amon, T.C.Y. Chan, *A new mathematical programming approach to optimize wind farm layouts*, Renewable Energy, **63**, pp. 674–680 (2014).